CrystEngComm

Cite this: *CrystEngComm*, 2012, **14**, 3446

www.rsc.org/crystengcomm

PAPER

Controlling anatase coating of diatom frustules by varying the binding layer†

Jeremiah Toster,[a] Catalin Harnagea,[b] K. Swaminathan Iyer,[a] Federico Rosei[b] and Colin L. Raston*[a]

Received 9th December 2011, Accepted 9th March 2012
DOI: 10.1039/c2ce06648c

Diatoms have ordered three dimensional porous exoskeletons (frustules) comprised primarily of amorphous silica which can be used as templates for materials applications. Hydrolysis of titanium(IV) isopropoxide (TIP) in the presence of surface bound poly(4-vinyl pyridine) or citric acid results in the formation of anatase on the surface after calcining at 450 °C, however as shown with atomic force microscopy (AFM), different morphologies are formed. Citric acid preferentially resulted in a thin film of anatase over the surface of the frustule whereas poly(4-vinyl pyridine) resulted in the formation of nano-particles of anatase (90–100 nm) on the surface.

1. Introduction

Diatoms are photosynthetic unicellular algae which are found in marine and fresh water environments.[1,2] They possess species specific porous exoskeletons comprised of silica, called frustules, as exemplified in Fig. 1. Diatoms are responsible for approximately one-fifth of the production of organic compounds from carbon dioxide on Earth as well as making up a quarter of all plant life by weight.[1,3] The frustules of diatoms provide an inexpensive avenue for access to complex 3-dimensional structures with a high level of precision at the nanoscale, with the spatial arrangement differing from one species to another. These porous 3-dimensional structures have potential applications in areas such as catalysis, solar cells, energy storage, sensors and drug delivery.[3–6]

Nature provides inspiration for many new technologies ranging from self cleaning surfaces to solar energy conversion devices.[7] Developing the use of the nanoporous structure of the frustules in the aforementioned applications depends on the ability to functionalise the silica with technologically relevant materials, such as titania, iron oxide and gold.[6,8–12] To this end we have investigated different strategies for coating frustules with titania, to develop a composite material with semiconducting properties while maintaining the high surface area and light trapping porous structure of the frustules. We find that poly(4-vinylpyridine) (P_4VP) or citric acid are effective in promoting and controlling the growth of the titanium(IV) material in different ways on the surface of the frustules from the hydrolysis of titanium(IV) isopropoxide (TIP), for the subsequent formation of anatase on calcining. P_4VP has previously been used to bind gold nanoparticles to the frustule surface specifically in the pores, and citric acid has been used to form thin film titania coated silica nanospheres similar to the thin films formed on the diatom frustules.[11,13] The common methods for coating titania on silica establish that the concentration of reagents affects the thickness of the deposited material, as does the number of cycles.[8,14–16] Most coatings involve the use $TiCl_4$ under controlled pH hydrolysis, as opposed to the use of TIP and water in the present study.[17,18] Wilhelm *et al.* coated silica nanoparticles using TIP, although here the particles were synthesised separately before being attached to the silica surface.[17] Diatom frustules have also been coated in a similar manner using phytic acid as a molecular binder for a prepared titania suspension.[19] Again pH control and adjustments are important, whereas in the present study using this approach but in the presence of P_4VP there is no requirement to adjust the pH for nanoparticle formation. Nevertheless the pH needs to be close to neutral because basic conditions are likely to result in dewetting and the P_4VP can act as an acid scavenger.[11,20]

Titania comes in three main forms, brookite, rutile and anatase of which anatase is best suited for technological applications possessing higher photocatalytic activity and better semiconducting properties.[21–23] Applications for titania include photovoltaics, particularly dye sensitised solar cells, photocatalysis, rocking chair lithium batteries, high dielectric capacitors in dynamic-random-access-memory (DRAM), and sensors.[24–27] The biosilification formation of the frustules themselves involves the 3D assembly of silica particles associated with surface roughness.[8] Losic *et al.* used atomic layer deposition to coat frustules with titania while controlling the pore size and increasing smoothness of the surface.[8]

Anatase titania is currently a major component for dye sensitised solar cells (DSSC's), which are currently the most efficient third generation solar cells.[28] Combining the porous structure of

[a]*Centre for Strategic Nano-fabrication, School of Chemistry and Biochemistry, University Of Western Australia, Crawley, WA-6009, Australia. E-mail: colin.raston@uwa.edu.au; Fax: +08 6488 8683; Tel: +08 6488 3045*
[b]*Institut National de la Recherche Scientifique, Université du Quebec, 1650 Boul. Lionel Boulet, J3X1S2 Varennes, QC, Canada. E-mail: rosei@emt.inrs.ca; Fax: +1 (450) 929 8102; Tel: +1 (514) 228 8246*

† Electronic supplementary information (ESI) available: Further AFM, complete XRD, complete SEM and EDS, TEM and FT-IR. See DOI: 10.1039/c2ce06648c

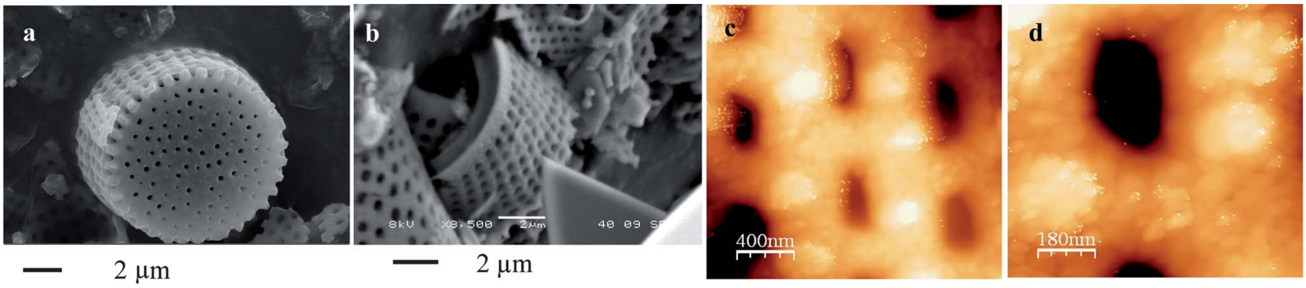

Fig. 1 Image of a diatom frustules surface. (a) SEM image of diatom frustule, (b) SEM image of the AFM tip approaching the frustule surface, (c and d) AFM images of a pristine diatom frustule in UHV taken in non-contact mode with a set point of 29.28 Hz.

the diatoms with high surface area titania nanoparticles has potential in improving the light harvesting ability of these cells.

2. Experimental

2.1 P_4VP coating

Diatom frustules were acquired from the Mount Sylvia mine in Queensland Australia and were cleaned using the GaLa Plasma Prep 5 air plasma chamber. Organic residues on the surface of the frustule were removed by ion bombardment without causing any observed damage to the underlying silica, thereby providing a pristine silica surface.[29] The plasma treatment was preferred over other methods commonly used for cleaning frustules which involve acid cleaning or piranha treatment, as it avoids the use of hazardous materials. A frequency of 40 kHz was applied for 5 min at a power setting of 110 W, then agitated to expose untreated regions and then similarly treated again twice more. Once cleaned, the diatom frustules (23.2 mg) were mixed with P_4VP (62.4 mg, Mw 60,000 Sigma Aldrich) dissolved in ethanol (100 mL) for 18 h to optimise surface coverage by the polymer. This concentration for the polymer was used as it was within the optimal range for particle immobilisation as shown by Malynych *et al.*[29] The frustules were then centrifuged, collected and found to have approximately a 20% increase in mass attributed to polymer attachment. They were then placed in an oven at 120 °C for four hours to stabilise the polymer coating,[29] followed by redispersing them in ethanol (5 mL) under nitrogen gas to control hydrolysis of titanium(IV) isopropoxide (TIP). This involved adding the titanium(IV) isopropoxide (TIP) (100 μL, Sigma Aldrich) with the stirred mixture exposed to air for 15 min which resulted in the formation of a white precipitate. Centrifugation was used to collect the hybrid titanium(IV)-silica material which was then calcined at 450 °C in air for four hours, resulting in the formation of anatase on the surface of the frustules.

2.2 Citric acid coating

Plasma cleaned diatom frustules (15.4 mg) were added to citric acid (50.2 mg, Analar) dissolved in ethanol (15 mL) and the resulting mixture stirred for two hours whereupon it was purged with nitrogen and TIP (30 μL) was added. This concentration of citric acid gave a 1 : 1 molar ratio of the acid to silica frustules, and decreasing the amount of silica any further has been shown to increase the quantity and size of pores on the titania film formed.[13] After 15 min a white precipitate was evident and the sample was then centrifuged and heated to 450 °C yielding frustules decorated with anatase particles.

Scanning electron microscopy (SEM) analysis was carried out using a Zeiss 1555 VP-FESEM instrument, and transmission electron microscopy (TEM) on a JEOL 3000F FEGTEM instrument, both housed in the Centre for Microscopy, Characterisation and Microanalysis at the University of Western Australia. Atomic force microscopy (AFM) was carried out on a JEOL 4500 ultra high vacuum (UHV) AFM/STM instrument with *in situ* SEM attachment at the Nano Femto Lab of INRS in Montreal, Canada.

3. Results and discussion

Plasma treated diatom frustules were analysed by AFM and SEM, with representative images displayed in Fig. 1. The results provide details of the rough surface in its pristine state. Fig. 1a–c show SEM and AFM images of the frustules present in the sample, revealing their shape and the intricate porous structure. Fig. 1b shows an SEM image of the AFM tip approaching the diatom giving a broad range of view of the area to be scanned. The AFM images (Fig. 1c–d) show the surface roughness which arises by the biosilification process involved in generating the frustules.[8] This roughness needs to be taken into account in identifying nanoparticles grown on the surface. The surface roughness of a pristine frustule makes it possible to image a continuous coating using AFM, noting a substantial build up of material will result in a smoothing effect on the surface. In the present study P_4VP and citric acid were used to encourage the formation of a layer of titanium rich material on the surface, with calcining at 450 °C generating anatase nanoparticles.

The main focus of the heat treatment is to ensure that all titania is in the crystalline anatase form which was confirmed by acquiring powder X-ray diffraction (XRD) patterns. Fig. 2(c) shows the major peak of the diffraction pattern at 25.40° which corresponds to the 101 Miller indices.[30] Other minor peaks at 37.92°, 48.12°, 54.12°, 55.20°, 62.80° and 65.04° correspond to known Miller indices of anatase respectively (004), (105), (200), (211), (204) and (116).[31] Using the Scherrer equation, which utilises the peak broadening effect that nanoparticles have on an XRD scan, an average particle size of 30–40 nm was extracted for the P_4VP sample. Frustules coated with titanium(IV) involving the use of P_4VP were analysed using both *in situ* SEM and AFM, with representative images presented in Fig. 3. AFM analysis of

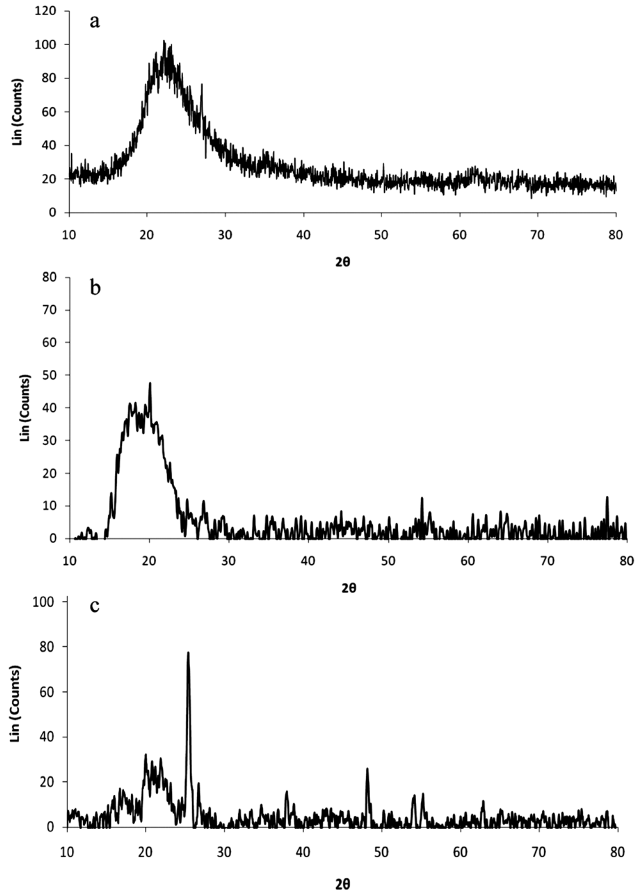

Fig. 2 XRD scans of (a) pristine diatom, (b) diatom coated with P_4VP and titania, (c) calcined diatom coated with P_4VP and titania.

the P_4VP sample before and post heat treatment show no obvious morphological difference (see ESI†). AFM indicates that there are some larger particles around 100 nm, however anything smaller than 40–50 nm is difficult to resolve due to tip convolution effects and some of the larger particles could also be clusters of smaller particles, and so the Scherrer equation gives a better overall picture of the average particle size. AFM shows a clear difference in arrangement and texture of particles of silica on the untreated frustules relative to that of anatase particles on the final material. EDS in Fig. 4 acquired from the SEM analysis confirms that titanium is present on the surface of a diatom using the citric acid and P_4VP methods (further details see ESI†). TEM images of the P_4VP derived samples (see ESI†) are very similar to images of pristine frustules (see ESI†) indicating that using standard TEM imaging is problematic for identifying particles on the surface of the frustules. Any regions of varying darkness may be due to thicker areas of the frustule and not necessarily due to the presence of titania. It is for this reason that AFM and SEM were primarily used for characterisation. XRD was carried out both before and after heat treatments of the frustules exposed to TIP (Fig. 2(b,c)), the former showing only a broad amorphous peak which is consistent with XRD of pristine diatoms shown in Fig. 2(a) indicating that the titanium(IV) material present is amorphous. After heat treatment (450–600 °C) peaks appear, clearly establishing the formation of the anatase phase of titania, and thus the hydrolysed titanium(IV) containing material on the surface is converted to the expected anatase phase under these conditions as shown in Fig. 2(c).[32]

The results from the citric acid coating technique are significantly different to those from the P_4VP coating technique. Fig. 3 shows that rather than forming particles on the surface of the frustule the citric acid is effective in promoting the formation of a uniform layer of titanium(IV). The AFM image in Fig. 3(f) shows a smoother surface than the untreated frustules in Fig. 3(d). As presented by Losic *et al.*,[8] the frustule showing less roughness on the surface can be representative of a coating which conceals much of the silica surface structure. The image in Fig. 3(f) was acquired after calcining at 450 °C, and it clearly establishes that the smooth surface is not associated with build up of citric acid which decomposes at much lower temperatures (approx 175 °C). Fig. 3(g–i) display line profiles of Fig. 3(d–f), presenting the surface topography resulting from the coating methods. The gradual variations in the height should not be attributed to the coatings but most likely to the natural curvature of the diatom surface. All line profiles are about 1 μm long and all show changing heights. As previously stated the natural roughness of the pristine diatom makes it possible to identify a thin film on the surface if there is a smoothing effect, as observed for the frustule presented in Fig. 3(i) which has been processed using the citric acid technique. Fig. 3(i) shows a smooth surface unlike the surfaces in Fig. 3(g–h). For Fig. 3(h) where the sample was prepared using the P_4VP technique, the maximum variation in height of the surface is 30 nm larger than that of pristine frustule (Fig. 3(i)). This large variation in the topography can be attributed to the 30–40 nm titania particles on the surface of the frustules.

P_4VP is well known for its ability to immobilise nanoparticles, including those of gold and silver,[33] and to act as a surface modifier for silica, metals and plastics.[11,29] The polymer can interact with the surface through silanol hydrogen bonding *via* the pyridyl groups resulting in strong binding to the silica surface, but with free pyridyl groups still available for surface binding, which can interact with nanoparticles of gold and silver.[29] Citric acid is capable of forming complexes with metal ions and is a known templating agent for strontium ferrite.[13,34] It is likely that citric acid has a strong hydrogen bonding interaction with the silica surface *via* the hydroxyl groups on both the acid and the plasma cleaned frustules. The formation of a monolayer or multiple layers of citric acid provides sites for complexing titanium(IV) ions in solution, either through primary or secondary coordination interactions. Presumably, when the titanium(IV) precursor is hydrolysed by water, titanium(IV) material deposits forms around the frustule, with the heat treatment then removing the citric acid along with any bridging hydroxo species between adjacent Ti(IV) centres as water molecules, with the formation of anatase on the surface.[13] FT-IR was carried out to determine the nature of the titanium(IV) material formed before calcination. However, the stretching bands of the silica diatoms masked the expected Ti–O and Ti–O–Si stretching bands (ESI†).[35,36] A control experiment was carried out in the absence of citric acid and P_4VP, which resulted in the formation of titania as anatase after calcining as randomly sized particles (80–400 nm) on the surface of the frustules (ESI†). These particles often cover the pores of the frustules, which we are

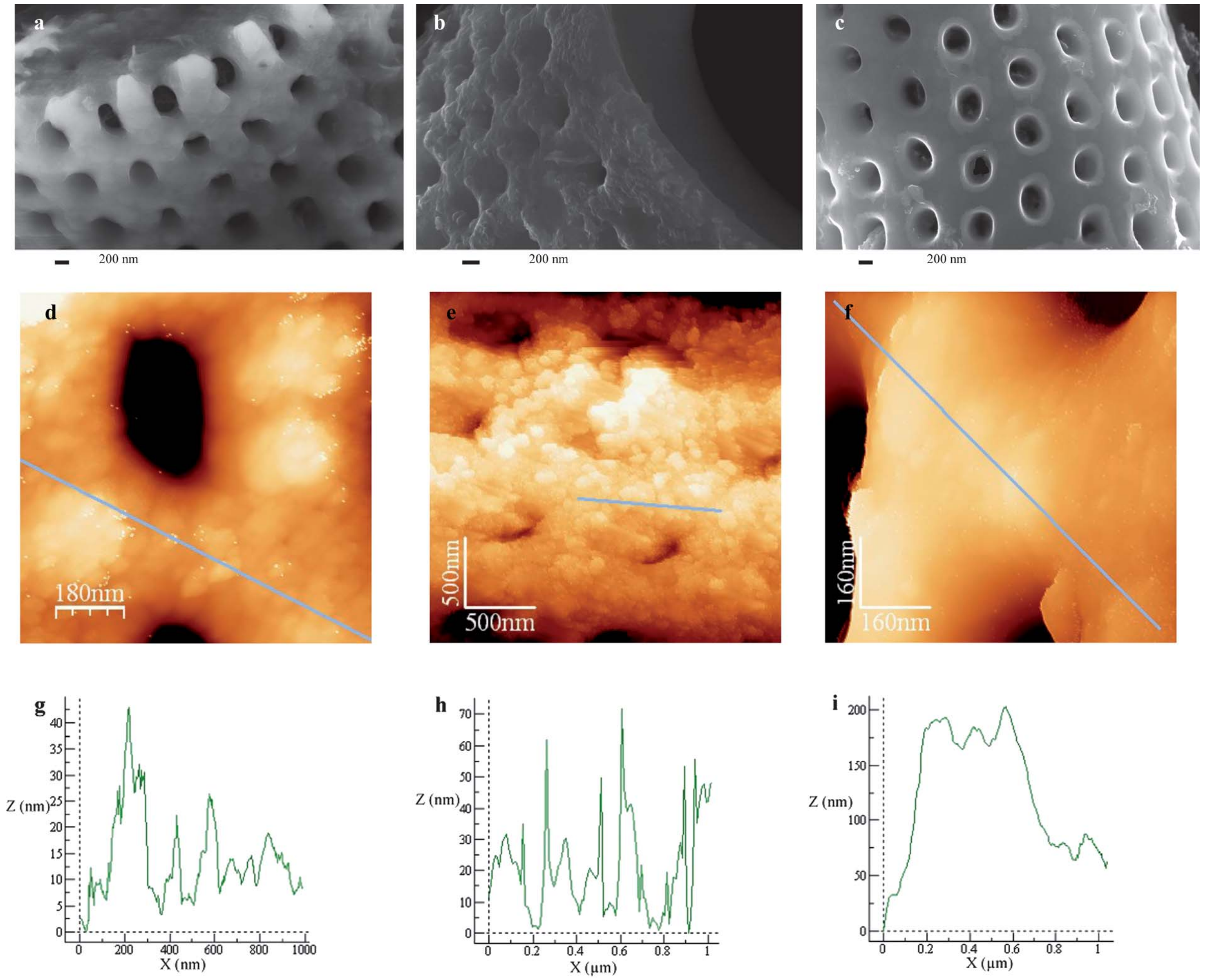

Fig. 3 SEM images, AFM images and line profiles of AFM images. (a,d,g) are of untreated frustules, (b,e,h) are of P_4VP treated frustules, (c,f,i) are of citric acid treated frustules. All AFM images were taken in non-conact mode with (d) and (f) having a set point of 29.28 Hz and (e) 46.36 Hz.

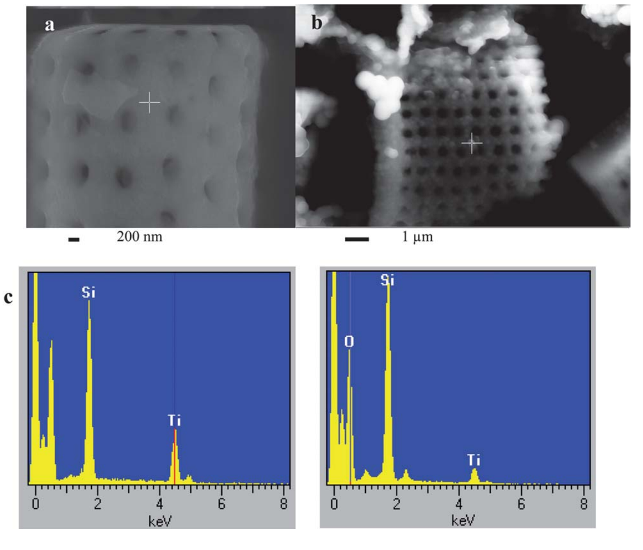

Fig. 4 (a) and (c) are SEM and EDS of titania coated diatom using citric acid, (b) and (d) are SEM and EDS of titania coated diatom using P_4VP.

attempting to preserve for light trapping and harvesting applications.

4. Conclusion

Other approaches for the processing of frustules to incorporate other materials such as zirconia, magnesium oxide and titania involve the use of high temperature displacement reactions, moulds of the frustules and a layer by layer deposition. We have developed a cheap and facile method of incorporating titania, either as a film or as particles, in a single process without effecting the three dimensional porous structure.[37,38] P_4VP and citric acid are both effective reagents in controlling the coating of the diatom frustules with titania, though their effect differs. AFM, SEM and TEM were used to analyse the frustule surfaces both before and after coating, with detailed information gathered on the coating using accurate SEM targeting of AFM tips. Surface modification using P_4VP resulted in the formation of predominantly less than 100 nm particles of titanium(IV) species on the surface of the frustule, which can be converted to anatase by calcining. In contrast citric acid resulted in a uniform layer of titanium(IV) material, and similarly titania after heat treatment.

In both cases there was no evidence for structural change to the frustule from plasma etching to calcining. The composite material based on anatase and silica has applications in DSSC's and photocatalysis. We note that 3D nanoporous frustules provide a built in light trapping feature for potentially improving current efficiencies of DSSC's, and this will be explored in further studies.

Acknowledgements

The authors graciously acknowledge the support of the Australian Research Council (ARC) and Mt Silvia Diatomite for the supply of diatoms. The SEM and TEM work was carried out at the Centre for Microscopy, Characterisation and Analysis (CMCA). F. Rosei is supported by NSERC (Discovery Grant) and is grateful to the Canada Research Chairs program for partial salary support. C. Harnagea is grateful to NSERC for a CGS scholarship. F. Rosei is grateful to UWA for a Gledden Visiting Fellowship (2008/2009) and for a Professor at Large Award (2010/2011) which fostered the collaboration.

Notes and references

1 C. Bowler, A. E. Allen, J. H. Badger and J. Grimwood, *et al.*, *Nature*, 2008, **456**, 239–244.
2 F. Noll, M. Sumper and N. Hampp, *Nano Lett.*, 2002, **2**, 91–95.
3 M. W. Anderson, S. M. Holmes, N. Hanif and C. S. Cundy, *Angew. Chem., Int. Ed.*, 2000, **39**, 2707–2710.
4 D. Losic, K. Short, J. G. Mitchell, R. Lal and N. H. Voelcker, *Langmuir*, 2007, **23**, 5014–5021.
5 D. Zhang, Y. Wang, J. Pan and J. Cai, *J. Mater. Sci.*, 2010, **45**, 5736–5741.
6 D. Losic, Y. Yu, M. S. Aw, S. Simovic, B. Thierry and J. Addai-Mensah, *Chem. Commun.*, 2010, **46**, 6323–6325.
7 A. Rinaldi, *EMBO Rep.*, 2007, **8**, 995–U993.
8 D. Losic, G. Triani, P. J. Evans, A. Atanacio, J. G. Mitchell and N. H. Voelcker, *J. Mater. Chem.*, 2006, **16**, 4029–4034.
9 N. L. Rosi, C. S. Thaxton and C. A. Mirkin, *Angew. Chem., Int. Ed.*, 2004, **43**, 5500–5503.
10 D. Losic, J. G. Mitchell and N. H. Voelcker, *New J. Chem.*, 2006, **30**, 908–914.
11 J. Toster, K. S. Iyer, R. Burtovyy, S. S. O. Burgess, I. A. Luzinov and C. L. Raston, *J. Am. Chem. Soc.*, 2009, **131**, 8356.
12 C. Jeffryes, T. Gutu, J. Jiao and G. L. Rorrer, *ACS Nano*, 2008, **2**, 2103–2112.
13 D. W. Lee, S. K. Ihm and K. H. Lee, *Chem. Mater.*, 2005, **17**, 4461–4467.
14 K. D. Kim, H. J. Bae and H. T. Kim, *Colloids Surf., A*, 2003, **224**, 119–126.
15 J.-H. Wu, X.-S. Li, Y. Zhao, Q. Gao, L. Guo and Y.-Q. Feng, *Chem. Commun.*, 2010, **46**, 9031–9033.
16 K. Schrijnemakers, N. Impens and E. F. Vansant, *Langmuir*, 1999, **15**, 5807–5813.
17 P. Wilhelm and D. Stephan, *J. Colloid Interface Sci.*, 2006, **293**, 88–92.
18 H. H. Choi, J. Park and R. K. Singh, *Appl. Surf. Sci.*, 2005, **240**, 7–12.
19 Y. X. Jia, W. Han, G. X. Xiong and W. S. Yang, *J. Colloid Interface Sci.*, 2008, **323**, 326–331.
20 B. J. Hritzko, M. J. Ortiz-Vega and N. H. L. Wang, *Ind. Eng. Chem. Res.*, 1999, **38**, 2754–2764.
21 M. Dolata, P. Kedzierzawski and J. Augustynski, *Electrochim. Acta*, 1995, **41**, 1287–1293.
22 Z. W. Wu and Y. F. Lu, *J. Sol-Gel Sci. Technol.*, 2010, **53**, 287–292.
23 B. H. Park, L. S. Li, B. J. Gibbons, J. Y. Huang and Q. X. Jia, *Appl. Phys. Lett.*, 2001, **79**, 2797–2799.
24 J. D. DeLoach, G. Scarel and C. R. Aita, *J. Appl. Phys.*, 1999, **85**, 2377–2384.
25 R. Hengerer, B. Bolliger, M. Erbudak and M. Grätzel, *Surf. Sci.*, 2000, **460**, 162–169.
26 J. Hong and S. W. Kang, *Ind. Eng. Chem. Res.*, 2010, **49**, 9124–9127.
27 H. W. Geng, R. X. Peng, S. K. Han, X. H. Gu and M. T. Wang, *J. Electron. Mater.*, 2010, **39**, 2346–2351.
28 M. Grätzel, *J. Photochem. Photobiol., C*, 2003, **4**, 145–153.
29 S. Malynych, I. Luzinov and G. Chumanov, *J. Phys. Chem. B*, 2002, **106**, 1280–1285.
30 F. Carn, A. Colin, M. F. Achard, H. Deleuze, C. Sanchez and R. Backov, *Adv. Mater.*, 2005, **17**, 62–66.
31 S.-J. Park, Y. C. Kang, J. Y. Park, E. A. Evans, R. D. Ramsier and G. G. Chase, *Journal of Engineered Fibers and Fabrics*, 2010, **5**, 50–56.
32 L. S. Hsu, R. Rujkorakarn, J. R. Sites and C. Y. She, *J. Appl. Phys.*, 1986, **59**, 3475–3480.
33 K. Kim, H. Ryoo and K. S. Shin, *Langmuir*, 2010, **26**, 10827–10832.
34 X. F. Yang, Q. L. Li, J. X. Zhao, B. D. Li and Y. F. Wang, *J. Alloys Compd.*, 2009, **475**, 312–315.
35 J. Bertaux, F. Frohlich and P. Ildefonse, *Journal of Sedimentary Research*, 1998, **68**, 440–447.
36 L. P. Xu, Y. X. Zhao, Z. G. Wu and D. S. Liu, *Chinese Chemical Letters*, 2003, **14**, 1159–1162.
37 K. H. Sandhage, S. M. Allan, M. B. Dickerson, C. S. Gaddis, S. Shian, M. R. Weatherspoon, Y. Cai, G. Ahmad, M. S. Haluska, R. L. Snyder, R. R. Unocic, F. M. Zalar, Y. Zhang, R. A. Rapp, M. Hildebrand and B. P. Palenik, *Int. J. Appl. Ceram. Technol.*, 2005, **2**, 317–326.
38 Y. Fang, Q. Wu, M. B. Dickerson, Y. Cai, S. Shian, J. D. Berrigan, N. Poulsen, N. Kröger and K. H. Sandhage, *Chem. Mater.*, 2009, **21**, 5704–5710.